One-pot synthesis of bi-disperse FePt nanoparticles and size-selective self-assembly into AB_2, AB_5, and AB_{13} superlattices†

Amandeep K. Sra,[a] Trevor D. Ewers,[a] Qiang Xu,[b] Henny Zandbergen[b] and Raymond E. Schaak*[a]

Received (in Berkeley, CA, USA) 3rd November 2005, Accepted 30th November 2005
First published as an Advance Article on the web 6th January 2006
DOI: 10.1039/b515673d

By chemically modifying the nucleation burst that generates monodisperse FePt nanocrystals, a mixture of Pt and Fe_xPt_{1-x} nanoparticles forms during a one-pot reaction that includes a small amount of Cu as a catalyst; size-selective precipitation yields a bi-disperse population of Fe_xPt_{1-x} nanoparticles, which can assemble into high-quality AB_2, AB_5, and AB_{13} superlattice structures.

The synthesis of uniform magnetic nanocrystals[1] and their self-assembly into periodic superlattices[2] is emerging as an attractive bottom-up strategy for accessing ordered sub-lithographic arrays with potential applications that include ultrahigh-density magnetic storage architectures[3,4] and spin-exchange magnets.[5] Binary superlattices are particularly attractive, as they can produce structures that are more complex than the standard close-packed hcp and fcc arrangements most frequently observed for single-component systems. In addition, binary superlattices have the potential to create new "metamaterials," which display unique collective properties that differ from their individual components.[6–8] To date, binary AB, AB_2, AB_5, and AB_{13} superlattices with the NaCl, AlB_2, $CaCu_5$, and $NaZn_{13}$ structure types, respectively, have been observed for physical mixtures of individually-synthesized nanoparticles with carefully-controlled size ratios and very narrow size distributions.[7–12]

Here, we present an alternative approach for forming binary nanoparticle superlattices. Instead of synthesizing the individual components and physically mixing them, we discovered that simple modifications to well-established reactions for generating monodisperse Fe_xPt_{1-x} nanoparticles[3,4,13] yield a mixture of phases with several size distributions. This one-pot mixture of nanoparticles can then be size-focused by controlled centrifugation to form a bi-disperse population of nanoparticles, which readily assemble into high-quality AB_2, AB_5, and AB_{13} superlattices. Such superlattices are still relatively rare, and the fact that they can be readily accessed using this unconventional method is important for gaining a better understanding of the range of conditions necessary to assemble them, as well as the structural details of the superlattices that form. In a more general sense, these results highlight the surprising degree of order that can emerge from complex one-pot reactions with seemingly disordered multi-modal particle size distributions, and will hopefully motivate continued synthetic exploration into other complex systems.

The synthesis (details in Supplementary Information†) was carried out using standard air-free techniques. In a typical synthesis, a 1 : 1 : 0.05 molar ratio of $Fe(acac)_3$, $Pt(acac)_2$, and $Cu(acac)_2$ was dissolved in octyl ether. 1,2-Hexadecanediol was added, and the reaction mixture was purged with argon. Oleic acid and oleylamine were then added to the reaction flask at room temperature before raising the reaction temperature to 250 °C and then subsequently lowering it to 210 °C. After 40 min, the solution was cooled to room temperature, and the nanoparticles were precipitated with ethanol. The product was isolated by centrifugation at 4000 rpm and washed several times.

TEM analysis of the product indicates the presence of three distinct types of particles: monodisperse 2.3 and 4.5 nm particles, along with polydisperse 10–20 nm particles (Fig. 1a). EDS analysis indicates that the largest particles are Pt, and these can easily be removed by centrifuging at 1000 rpm. After re-suspending the purified precipitate in hexane and centrifuging at 1000 rpm for 6 min, the product contains exclusively a bimodal distribution of the smaller 2.3 and 4.5 nm particles (Fig. 1b). Drop-casting the colloidal solution containing 2.3 and 4.5 nm particles in hexane, followed by slow evaporation of the solvent, yields three types of two-dimensional superlattices (Fig. 1c): AB_2, AB_5, and AB_{13}, which match the AlB_2, $CaCu_5$, and $NaZn_{13}$ structure types, respectively.[14] For slower centrifugation speeds (1000 rpm) and shorter times, the AB_2 and AB_5 superlattices predominate. Higher centrifugation speeds (4000 rpm) and longer times significantly enrich the sample in the smaller 2.3 nm particles, allowing the AB_{13} superlattice to form preferentially.

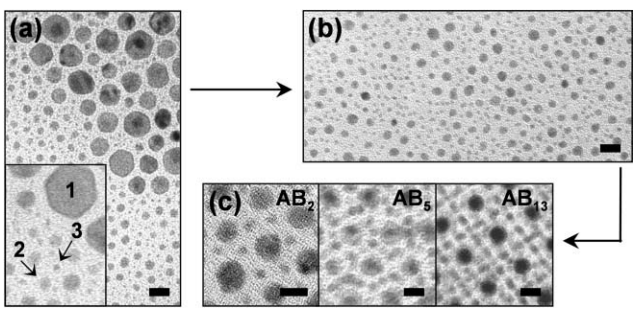

Fig. 1 TEM micrographs of (a) as-synthesized (1) 10–20 nm Pt, (2) 4.5 nm Fe_xPt_{1-x}, and (3) 2.3 nm Fe_xPt_{1-x} nanoparticles, (b) bi-disperse sample (2.3 and 4.5 nm particles) obtained after removing larger Pt particles by centrifugation, and (c) AB_2, AB_5, and AB_{13} superlattices assembled after further size selection *via* centrifugation. Scale bars represent 10 nm in (a) and (b) and 5 nm in (c).

[a]*Department of Chemistry, Texas A&M University, College Station, TX 77842-3012, USA. E-mail: schaak@mail.chem.tamu.edu*
[b]*Laboratory for Materials Science, National Centre for HREM, Delft University of Technology, Rotterdamseweg 137, 2628 AL, Delft, The Netherlands*

† Electronic supplementary information (ESI) available: Complete synthesis details, particle size distribution data, and representative EDS data. See DOI: 10.1039/b515673d

TEM micrographs of the AB_2 and AB_5 superlattices, along with their intermetallic AlB_2 and $CaCu_5$ prototypes, are shown in Fig. 2. In both structures, the 4.5 nm particles form a hexagonal lattice surrounded by the 2.3 nm particles. The primary differences between the two structures are the layer sequences and the number of 2.3 nm particles surrounding each 4.5 nm particle, which is greater in the AB_5 lattice. The AB_{13} superlattice, shown in Fig. 3, has a cubic arrangement of 4.5 nm particles surrounded by an icosahedron of 2.3 nm particles, as well as an additional 2.3 nm particle in the center of the unit cell. The unit cell obtained from the nanoparticle superlattice matches well with that expected for the intermetallic $NaZn_{13}$ structure (Fig. 3e). These AB_2, AB_5, and AB_{13} structures have been previously observed in binary nanoparticle superlattices,[7–12] although only for highly monodisperse physically-mixed samples.

Interestingly, we observe both the $NaZn_{13}$-type AB_{13} structure with an icosahedral packing of the smaller B spheres (Fig. 3f), as well as the recently reported cubic AB_{13} structure with a unique cubic arrangement of the B spheres (Fig. 3g). The cubic AB_{13} structure has a lower packing density than the icosahedral polymorph and is not known in bulk-scale intermetallic systems, but was recently observed in physical mixtures of PbSe and Pd nanoparticles.[8] Our results highlight the prevalence of this new structure type, and show that it can exist in thin samples that are nearly two dimensional (*e.g.* appear to be only 1–2 unit cells thick) and for a size ratio that is somewhat smaller than previously observed ($r_B/r_A = 0.511$).

The Fourier transforms in Figs. 2c and 3b confirm the long-range order of the hexagonal AB_5 and cubic AB_{13} superlattices, respectively. Likewise, the selected-area electron diffraction pattern in Fig. 3c shows a single-phase fcc structure, which is consistent with the Fe_xPt_{1-x} alloy nanoparticles. The particles that comprise the AB_2 superlattices were found to be 4.1 ± 0.4 nm $Fe_{52(12)}Pt_{48(12)}$ and 2.1 ± 0.2 nm $Fe_{54(12)}Pt_{46(12)}$, while the AB_5 superlattices were comprised of 4.5 ± 0.3 nm $Fe_{52(12)}Pt_{48(12)}$ and 2.3 ± 0.2 nm $Fe_{54(12)}Pt_{46(12)}$ particles. The AB_{13} superlattices consist of 4.5 ± 0.4 nm $Fe_{46(9)}Pt_{54(9)}$ and 2.3 ± 0.2 nm $Fe_{42(8)}Pt_{58(8)}$. (The deviations in particle size were determined by statistical analysis of more than 100 individual nanoparticles for each sample; details are included as Supplementary Information.† The values in parentheses are the standard deviations of the composition measurements, derived from EDS analysis of more than 50 individual particles of each type.)

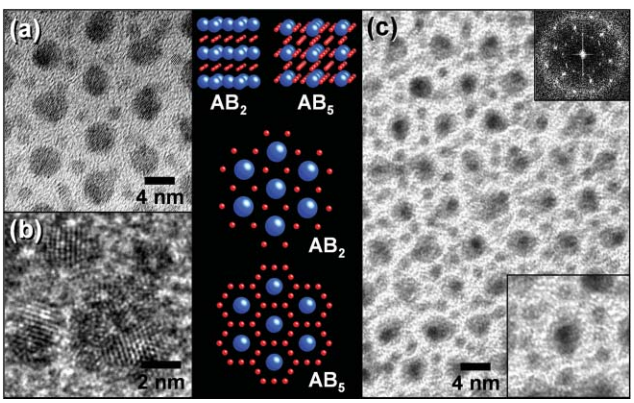

Fig. 2 TEM micrographs of (a, b) AB_2 and (c) AB_5 nanoparticle superlattices comprised of 4.5 and 2.3 nm Fe_xPt_{1-x} particles. Lattice fringes in (b) highlight the nanoparticle crystallinity. The intermetallic AB_2 (AlB_2) and AB_5 ($CaCu_5$) crystal structures are shown in the center for comparison. The upper inset in (c) shows the Fourier transform, highlighting the long-range order of the superlattice, and the lower inset shows the 4.5 nm central particle surrounded by twelve 2.3 nm particles, which is characteristic of the AB_5 structure.

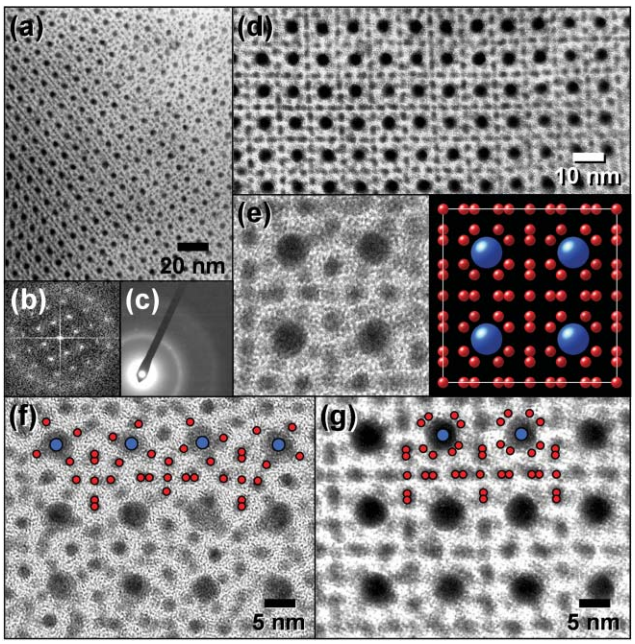

Fig. 3 TEM micrographs of AB_{13} nanoparticle superlattices. Panel (a) shows a large-area superlattice. (b) The corresponding Fourier transform highlights the cubic long-range ordering, and (c) the selected-area electron diffraction pattern shows the fcc structure of the Fe_xPt_{1-x} nanoparticles that comprise the superlattice. An extended lattice of several unit cells is shown in (d), and a single unit cell is shown in (e), along with the crystal structure of the intermetallic $NaZn_{13}$ structure. Panels (f) and (g) highlight the differences between the standard icosahedral AB_{13} structure (f) and the cubic AB_{13} polymorph (g) that was recently reported by Murray and co-workers.[8] Both polymorphs appear in our samples.

Our synthetic approach, which yields a mixture of several types of particles that ultimately lead to a bi-disperse sample of Fe_xPt_{1-x}, differs from other routine syntheses of FePt nanoparticles[3,4,13] in two primary ways. First, all of the reagents are added together at room temperature rather than after heating, which modifies the nucleation burst that typically leads to monodisperse particles.[15] Second, a small amount of Cu^{2+} is added to the reaction, which also likely modifies the nucleation burst and contributes to the multiple types of particles. Samples with no Cu^{2+} yielded only 2.2 ± 0.2 nm FePt particles. We speculate that Cu^{2+} reduces before Fe^{3+}, and the limited amount of reduced Cu helps to catalyze the formation of a population of Fe_xPt_{1-x} nanoparticles with a size that is different from the standard value. This argument is based on reduction potentials, known kinetics of reduction, and knowledge from similar systems that excess Fe or a strong reducing agent is needed to form $Fe_{50}Pt_{50}$ nanoparticles.[13] A small amount of Cu was detected in the nanoparticle samples (see Supporting Information†), but not reproducibly. Thus, it is difficult to discern whether Cu is actually incorporated into the FePt nanoparticles. This is not unusual for systems where small percentages of nanoparticle seeds are used in a

reaction, as their identification often remains elusive.[16] (In many cases reported in the literature, seeds and low-level metal impurities, which are not reproducibly detected in the final products, are known to change the nanoparticle shape and size.[16])

In summary, binary AB_2, AB_5, and AB_{13} Fe_xPt_{1-x} nanoparticle superlattices were isolated by controlled centrifugation of a one-pot reaction that generates a multi-modal distribution of particles. While the exact formation mechanism remains unknown, the results clearly indicate that subtle modifications to nanocrystal synthetic strategies can be exploited to yield complex multi-modal systems that can be cleaned up to generate well-ordered nanoparticle superlattices. Furthermore, the observation and analysis of high-quality binary nanoparticle superlattices in this system represents an important addition to our growing knowledge of this new class of nanostructured materials. More detailed studies are in progress to understand the effect of Cu concentration on the nucleation and growth of the nanoparticles, as well as attempts to convert the surface-confined alloy-type Fe_xPt_{1-x} nanoparticle superlattices into the technologically-relevant $L1_o$ structure.

This work was supported by startup funds from Texas A&M University and funding from the Robert A. Welch Foundation (Grant No. A-1583). Acknowledgment is also made to the donors of the Petroleum Research Fund, administered by the American Chemical Society, for partial support of this work. Electron microscopy was performed at the Microscopy and Imaging Center at Texas A&M University. The work at Delft was supported by the Nederlandse Stichting voor Fundamenteel Onderzoek der Materie (FOM).

Notes and references

1 T. Hyeon, *Chem. Commun.*, 2003, 927–934.
2 A. L. Rogach, D. V. Talapin, E. V. Shevchenko, A. Kornowski, M. Haase and H. Weller, *Adv. Funct. Mater.*, 2002, **12**, 653–664.
3 S. Sun, C. B. Murray, D. Weller, L. Folks and A. Moser, *Science*, 2000, **287**, 1989–1992.
4 S. Sun, S. Anders, T. Thomson, J. E. E. Baglin, M. F. Toney, H. F. Hamann, C. B. Murray and B. D. Terris, *J. Phys. Chem. B*, 2003, **107**, 5419–5425.
5 H. Zeng, L. Ling, J. P. Liu, Z. L. Wang and S. Sun, *Nature*, 2002, **420**, 395–398.
6 A. L. Rogach, *Angew. Chem., Int. Ed.*, 2004, **43**, 148–149.
7 F. K. Redl, K. S. Cho, C. B. Murray and S. O'Brien, *Nature*, 2003, **423**, 968–971.
8 E. V. Shevchenko, D. V. Talapin, S. O'Brien and C. B. Murray, *J. Am. Chem. Soc.*, 2005, **127**, 8741–8747.
9 C. J. Kiely, J. Fink, M. Brust, D. Bethell and D. J. Schiffrin, *Nature*, 1998, **396**, 444–446.
10 C. J. Kiely, J. Fink, J. G. Zheng, M. Brust, D. Bethell and D. J. Schiffrin, *Adv. Mater.*, 2000, **12**, 640–643.
11 E. V. Shevchenko, D. V. Talapin, A. L. Rogach, A. Kornowski, M. Haase and H. Weller, *J. Am. Chem. Soc.*, 2002, **124**, 11480–11485.
12 A. E. Saunders and B. A. Korgel, *ChemPhysChem*, 2005, **6**, 61–65.
13 K. E. Elkins, T. S. Vedantam, J. P. Liu, H. Zeng, S. Sun, Y. Ding and Z. L. Wang, *Nano Lett.*, 2003, **3**, 1647–1649.
14 J. V. Sanders and M. J. Murray, *Philos. Mag. A*, 1980, **42**, 721–740; J. V. Sanders, *Philos. Mag. A*, 1980, **42**, 705–720.
15 C. B. Murray, D. J. Norris and M. G. Bawendi, *J. Am. Chem. Soc.*, 1993, **115**, 8706–8715; C. B. Murray, S. Sun, W. Gaschler, H. Doyle, T. A. Betley and C. R. Kagan, *IBM J. Res. Dev.*, 2001, **45**, 47–56.
16 N. R. Jana, L. Gearheart and C. J. Murphy, *Adv. Mater.*, 2001, **13**, 1389–1393; S. Chen, Z. L. Wang, J. Ballato, S. H. Foulger and D. L. Carroll, *J. Am. Chem. Soc.*, 2003, **125**, 16186–16187; Y. Xiong, J. Chen, B. Wiley, Y. Xia, Y. Yin and Z.-Y. Li, *Nano Lett.*, 2005, **5**, 1237–1242; B. Wiley, Y. Sun and Y. Xia, *Langmuir*, 2005, **21**, 8077–8080.

